Heat transfer performance and influences of spray cooling under quenching

*Nianyong ZHOU, Hao FENG, Muhao XU, Enhai LIU**

College of Petroleum Engineering, Changzhou University, Changzhou 213164, Jiangsu, China

*Corresponding author: E-mail: liuenhai1018@126.com

Abstract: In this study, a closed-loop spray cooling system using R134a as the working fluid was established. The heat transfer characteristics and influencing mechanism of transient spray cooling were studied. The transient spray cooling curve under quenching was built accurately. The results show that the vapor film suppressed time t_{sup} is the main period that the spray cooling must pass through. The flow rate and the sub-cooling of R134a have little effect on the cooling rate but the critical heat flux, which are mainly affected by chamber pressure. The transient Jacob number Ja^* decreases with the increases of chamber pressure. As Ja^* decreases, the growth of vapor film is inhibited, then the t_{sup} reduces in consequence. The surface temperature drop point and critical heat flux increases with the rise of chamber pressure. The maximum critical heat flux is 70.08 W/cm^2 in this experiment.

Keywords: Transient spray cooling, Surface heat transfer, Cooling rate, Surface temperature drop

1.Introduction

Spray cooling is an efficient heat transfer technology that atomize working fluid under certain pressure and spray it onto a heat sink surface to remove heat. Compared with conventional heat dissipation methods, spray cooling has numerous advantages such as low heat transfer temperature difference, less flow rate demand, high heat flux and uniform temperature distribution [1].

Today, transient heat transfer involving in many fields: medical field, metallurgy, microelectronics, machining, aerospace and other fields [2-5]. In medical field, it is used to prevent skin or tissues from injury during high power laser therapy [6]. In metal heat treatment, the quenching of workpiece at the high initial temperature is a typical transient cooling process. The application of spray cooling technology will improve the rate and quality of quenching [7]. The rapid cooling of electronic chip after overtemperature is to prevent the equipment from damage in continuous high temperature [8]. The cooling process of laser weapon in intermittent operation [9]. In these conditions, how to improve the cooling rate of the equipment is of great attention. As of today, studies in transient spray cooling is relatively insufficient, which requires further improvement.

Spray cooling involves complex multiphase flow progress, and the heat transfer mechanisms and influence factors of which are relatively abundant. Cabrera et al. [10] investigated the effects of droplet Sauter mean diameter, droplet velocity, ambient pressure, surface roughness and other factors on heat flux using water as the working fluid, and a series of empirical formulas were proposed to describe the nucleate boiling and critical heat flux. Xie et al. [11] studied the heat transfer performance of enhanced structure surfaces in spray cooling. They found that besides enhancing the heat transfer, macro-structured surfaces also give other advantages in reducing the duration when the heater surface

remains in the high temperature regime (which is the film boiling stage in this study) after switching off the power. Chen et al. [12] discovered that the droplet velocity has the major effect on critical heat flux (CHF), followed by droplet flux. The influence of the Sauter mean diameter was negligible. Peng et al. [13] used R21 as the working fluid to study the heat transfer performance of transient spray cooling and obtained the regulation of surface temperature with the change of initial surface temperature. They also found that in nucleate boiling regime, heat flux at given surface temperature increases with the spray flow rate, and has a maximum value with nozzle-to-heater distance. Hsieh et al. [14] employed R134a as the working fluid to investigate the effects of mass flux, Weber number and sub-cooling on the process of cooling the circular surface with a full cone or circular nozzle. Liu et al. [15] studied the heat transfer performance of diverse microstructure surfaces, and it was concluded that the heat transfer enhanced mechanism of microstructure was mainly related to the surface area, compactness and arrangement, and the increase of surface area was the main factor. Cao et al. [16] established a closed-loop spray cooling system using R134a as the working fluid to study the cooling performance under different mass flow rate, chamber pressure and heat flux. The result shows that the experiment has the excellent heat transfer performance and the maximum CHF reached 130W/cm^2 while the surface temperature could be controlled below 45℃. Lu et al. [17] investigated the effects of spray height, flow rate and other factors on the heat transfer performance of spray cooling based on the numerical results. Liu et al. [18] enhanced the spray cooling performance by adding different proportion of ethanol and n-butanol into water. The results reveal that the performance of spray cooling is gradually enhanced with increasing concentration before the optimum concentration. Rini et al. [19,20] studied nucleation density, growth and life cycle of bubbles in spray cooling using FC-72 as the working fluid. The results declared that bubbles formation process in spray cooling was alike to that in pooling boiling. Tian et al. [21] observed the similarity of dynamic heat flux with different cryogens, nozzles, and substrates, and proposed a dimensionless correlation by the spray Biot number. Liu et al. [22] studied the influence of air on a closed-loop spray cooling process. The results show that the spray cooling is mainly affected by the liquid subcooling and surface superheat when air is present. The chamber total pressure has a negligible influence on the spray cooling heat transfer, which differs from the spray cooling behavior without air.

In recent years, lots of scholars have engaged in the field of spray cooling. However, most of these studies were about steady state, being short of the researches on transient spray cooling. In this paper, the closed-loop spray cooling system was set up to study the transient heat transfer process of spray cooling. From a review of proposed studies, the effects of flow rate, sub-cooling and chamber pressure on the spray cooling process were investigated. The physical mechanism and method of improving spray rate were explored.

2.Experiment

2.1. Experimental system

Fig. 1 shows the closed-loop spray cooling system in this study, which mainly consists of a spray chamber, a heating system, a liquid-giving system and a data acquisition system. Its operation process is as follows: first the gaseous working fluid flowed out of the gas-liquid separator, then compressed by the compressor and entered the pre-cooler for preliminary cooling. Later it was condensed to the subcooled liquid in the condenser. After the subcooled working fluid passed through the flow meter, it

would be sprayed onto the top surface of the experiment block by the nozzle. The well-atomized droplets impacted the top surface and evaporated to remove a great deal of heat. Then the working fluid entered the pre-cooler to absorb heat to ensure that the working medium is gaseous. Before flowing back to compressor for next cooling cycle, the gaseous working fluid flowed through the water cooler to ensure the working fluid temperature meet the requirement of the compressor inlet temperature.

According to the research results of Liu et al. [22], to eliminate the influence of air in the exploration experiments of the effect of the chamber pressure on heat transfer, the spray system should be vacuumed before charging the R134a in this study. In each of the experimental conditions, the heating system should be started first. When the temperature measuring points T_1 reaches to the initial cooling temperature, heating system should be turned off and the spray cooling system be started immediately.

R134a and R410A are extensively used in many kinds of the spray cooling systems due to their high latent heat, low boiling point, zero ozone depletion potential and low global warming potential. However, R410A requires higher operating pressure because of its lower boiling point. Considering the safe operation of the system, R134a was selected as the working fluid in the experiment due to its relatively high latent heat and boiling point (217.0 kJ/kg and -26.1 ℃ respectively at ambient atmosphere).

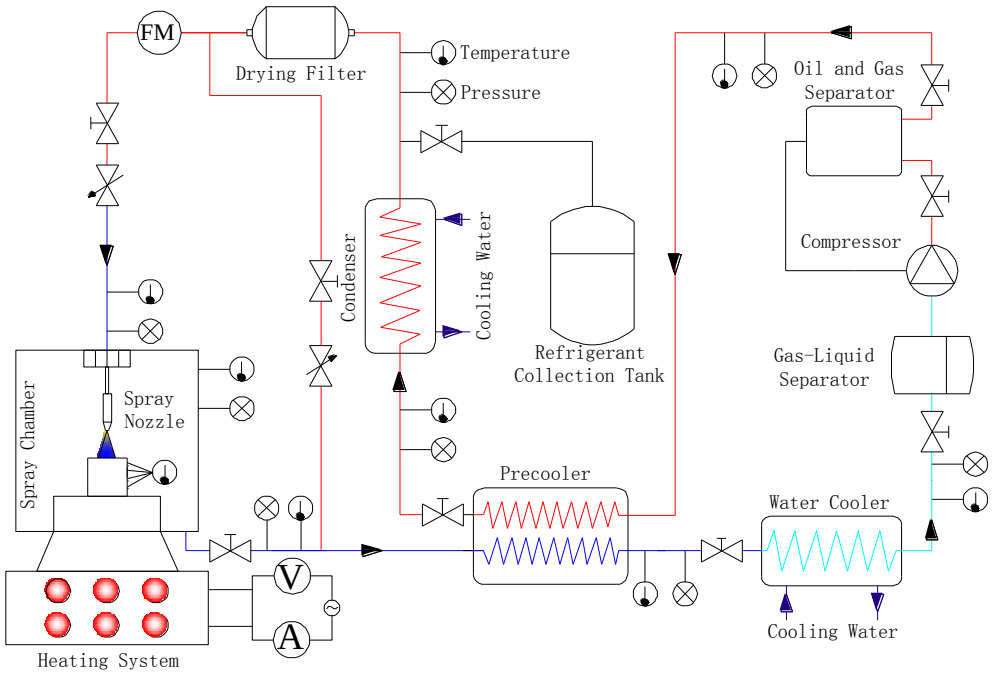

Fig. 1 Schematic of the closed-loop spray cooling experimental system

2.2. Spray chamber and Heat source

The structure of spray chamber designed in present work is shown in Fig.2. The chamber is well sealed and its upper limit pressure is about 10 bar. The whole chamber (except for the observation window) was isolated from surrounding environment by the thick aluminum silicate fiber cotton. The thickness of the observation window is 15 mm, which is used to observe the spray state. A spray nozzle (Spraying System Co. 1/8GG-SS3002.5) was installed in the top of the spray chamber,

adjoining by a height adjustment device that could alter the spray distance between nozzle and the top surface of the experiment block. This type of nozzle has several advantages including good corrosion resistance and uniform distribution of spray droplets.

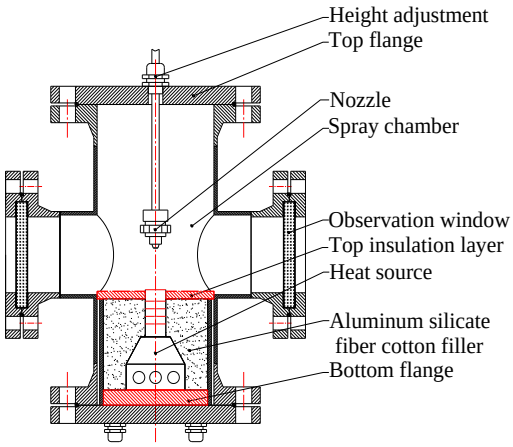

Fig. 2 Structure of the spray chamber

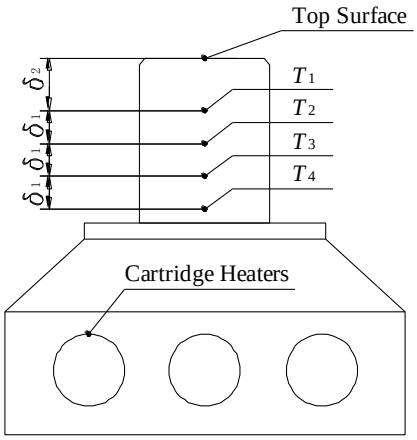

Fig. 3 Structure of the heat source

Fig. 3 illustrates the structure of heat source which is pure copper. Installing the K-type thermocouples to the experiment block, the points are named as T_1 T_2 T_3 and T_4. The diameter of the top surface is 24 mm. The heating power is controlled by an intelligent parameter acquisition device (PW9901) and its range is 0 to 1500 W.

2.3. Uncertainty analysis of measuring instruments

The accuracy of the measuring devices used in the experiment are shown in Table. 1.

Tab.1

Measurement data and accuracy of devices

Measurement data	Devices	Range	Uncertainties
Chamber temperature	PrT (PT100)	-50-150 ℃	± 0.15 ℃
Heat source temperature	thermocouple (K-type)	0-800 ℃	± 0.004 |T|
Spray inlet pressure	Pressure sensor	0-1.6 MPa	± 0.25 % FS
Flow rate	Liquid turbine flowmeter	0-10 L/min	± 1 %

According to the error transfer formula [23], the uncertainty of heat flux and temperature of the top surface in the experiment are ± 5.6 % and ± 2.9 %. The random error formulas in this paper are as follows:

$$\Delta q=\sqrt{\left(\frac{\partial q}{\partial T_1}\Delta T_1\right)^2+\left(\frac{\partial q}{\partial T_2}\Delta T_2\right)^2+\left(\frac{\partial q}{\partial \delta_1}\Delta \delta_1\right)^2+\left(\frac{\partial q}{\partial t}\Delta t\right)^2} \tag{1}$$

$$\Delta T_w=\sqrt{\left(\frac{\partial T_w}{\partial T_1}\Delta T_1\right)^2+\left(\frac{\partial T_w}{\partial q}\Delta q\right)^2+\left(\frac{\partial T_w}{\partial \delta_2}\Delta \delta_2\right)^2} \tag{2}$$

3. Data Process

3.1. Data calculation

Good insulation measures were taken on the circumferential side of the experiment block. Therefore, the temperature distribution of the experiment block follows the one-dimensional transient heat conduction in the axial direction [13]. In addition, the heat capacity is taken into consideration in the transient spray cooling state. Heat flux dissipated by transient spray can be obtained by:

$$q = \lambda \frac{T_2 - T_1}{\delta_1} - \delta_1 \rho c_p \frac{\Delta T_1}{\Delta t} \tag{3}$$

where ρ, c_p and λ are the density, specific heat capacity and thermal conductivity of experiment block, δ_1 is the distance between T_1 and T_2, ΔT_1 is the temperature difference of Δt.

The top surface temperature can be calculated by:

$$T_w = T_1 - q \frac{\delta_2}{\lambda} \tag{4}$$

where T_w is the temperature of the top surface, δ_2 is the distance between T_w and T_1.

In closed-loop spray cooling, the cooling performance in boiling regime is mainly influenced by dimensionless parameters such as Prandtl number *Pr* and Jacob number *Ja* [24,25]. Ja represents the superheat of vapor film in boiling heat transfer. The larger Ja is, the easier the refrigerant impinging on the top surface vaporizes to form a patchy area of vapor film, which inhibits the heat transfer. The *Ja* is the ratio between cooling capacity provided by sub-cooling and latent heat, and *Pr* represents the ratio between momentum diffusion capacity and thermal diffusion capacity, which are expressed as:

$$Ja^* = \frac{c_p (T_c^t - T_{sat})}{\gamma_{lh}} \tag{5}$$

$$Pr = \frac{c_p \mu}{\lambda} \tag{6}$$

where T_c^t is the transient chamber temperature, γ_{lh} is the latent heat, T_{sat} is the saturation temperature

3.2. Reliability verification

According to inverse heat conduction problem method (IHCP) [26], the differential equations and boundary conditions of experiment block was established, and the integral equations of interior, top surface and bottom were discretized in time and space. At last, the integral equations were converted into matrix form and then solved by MATLAB software.

In the process of verification, the top surface heat transfer coefficients under various conditions are fitted based on the experimental data. The temperature of 4 points (T_1', T_2', T_3' and T_4') calculated by IHCP are compared with the experimental values (T_1, T_2, T_3 and T_4). If the errors are in the range, the heat transfer coefficients could be applied. Otherwise, these would be adjusted until the errors are allowed. Then the top surface temperature (T_w') calculated by IHCP are compared with the temperature (T_w) calculated by the Eq. (3) and Eq. (4). When the deviations of them are in the range, the solution method proposed in this paper could be applicable. The verification processing is shown in Fig. 4.

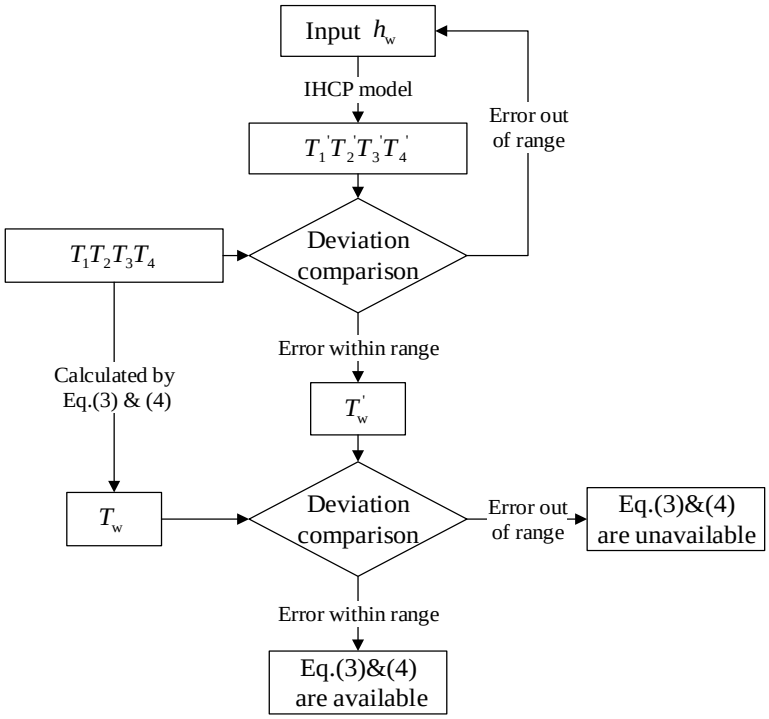

Fig. 4 Verification flowchart of the two calculation methods

An example of verification process is as follows:

At first, the errors between the experimental values and IHCP were compared，the results are shown in Fig. 5. It can be seen the mean relative error between IHCP and the experimental values are very small, so the heat transfer coefficients of the top surface are reliable. Further, T_w' and T_w were compared and the contrastive result is shown in Fig. 6.

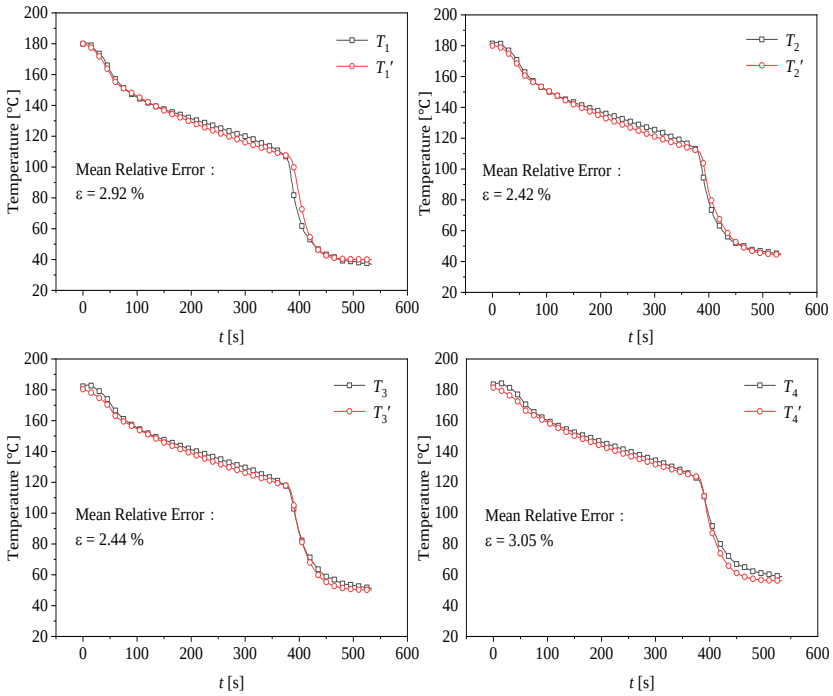

Fig. 5 Comparison between the solution of IHCP and the experimental values

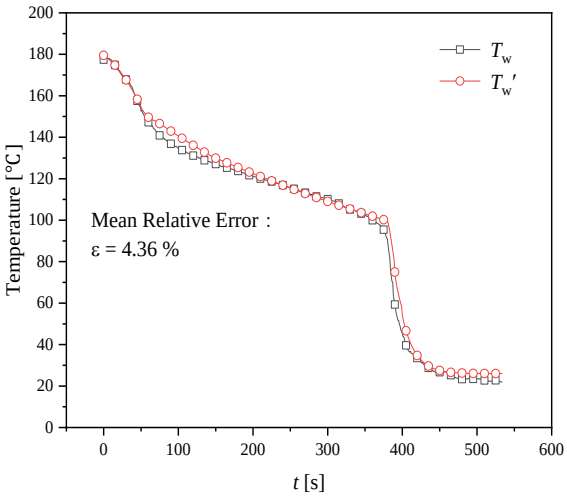

Fig. 6 Comparison between T_w' and T_w

It can be seen the mean relative error is merely 4.36%. Above all, it is practicable to use the Eq. (3) & (4) to calculate the heat flux and top surface temperature.

4. Results and Discussions

4.1. Analysis of transient spray cooling curve

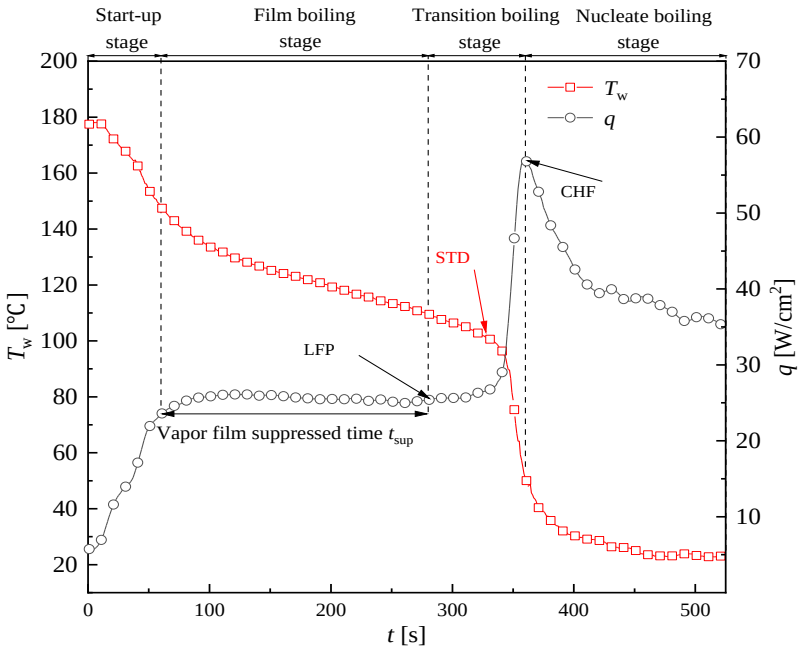

Fig. 7 Closed-loop transient spray cooling experiment curve

As is shown in Fig. 7, the curves of heat flux and top surface temperature are established when the flow rate Q is 0.19 L/min. As observed from Fig. 7, the closed-loop transient spray cooling curve in the experiment contains four stages: Start-up stage, Film boiling stage, Transition boiling stage and Nucleate boiling stage.

In the start-up stage, the top surface temperature drops at a fast speed and the heat flux increases significantly. The reason of the obvious heat transfer enhancement is that a stable vapor film has not been formed on the top surface at the initial stage of spray cooling. Besides, with the increase of flow

rate in the beginning, the cooling capacity is strengthened in a short time. And the duration of this stage is about 60 s in this experiment curve.

In film boiling stage, due to the relatively high surface temperature, the working fluid vaporizes extensively to form the vapor film, so that the heat transfer is suppressed. In this stage, the heat flux and temperature of the top surface decreases slowly with the increase of vapor film thickness. When the heat flux decreases to Leiden Frost point LFP where T_w is 112.3 ℃, q is 25.0 W/cm^2.The spray cooling immediately enters transition boiling stage. In the early of transition boiling stage, the change of heat flux and top surface temperature are all not obvious. In the later stage, the top surface temperature reaches the surface temperature drop point (STD), which is 100.8 ℃. Nucleate boiling will gradually take the place of film boiling and becomes the main heat transfer mechanism. Meanwhile, with the rapid increase of heat flux, the top surface temperature drops sharply.

The spray cooing process starts to enter nucleate boiling stage when the heat flux increases to the critical heat flux (CHF), which is 56.5 W/cm^2. Then the heat flux decreases to be steady, and the top surface temperature also decreases to be steady after a momentary sharp decrease. The process turns to the single-phase regime after the top surface temperature drops below the saturation temperature of R134a. Due to the temperature decreases very slowly in the late stage of nucleate boiling, it would take a lot of time to pass through the single-phase regime. And the application value of single-phase regime of R134a is relatively low. Therefore, the heat transfer in the single-phase regime is not considered in the paper.

Above all, the time of the refrigerant vapor film on the top surface suppressing the heat transfer, which is called the vapor film suppressed time t_{sup} , is the main period that the spray cooling should go through. The physical mechanism to increase the cooling rate is to reduce the vapor film suppressed time t_{sup} that the further reason is the thickness of vapor film. Therefore, the effects of flow rate, sub-cooling, chamber pressure and its influencing mechanism were given below.

4.2. Effect of flow rate on heat transfer process

In the experiment, by adjusting the valve opening to change the flow rate of R134a, the characteristics of top surface temperature and heat flux in transient spray cooling are analyzed.

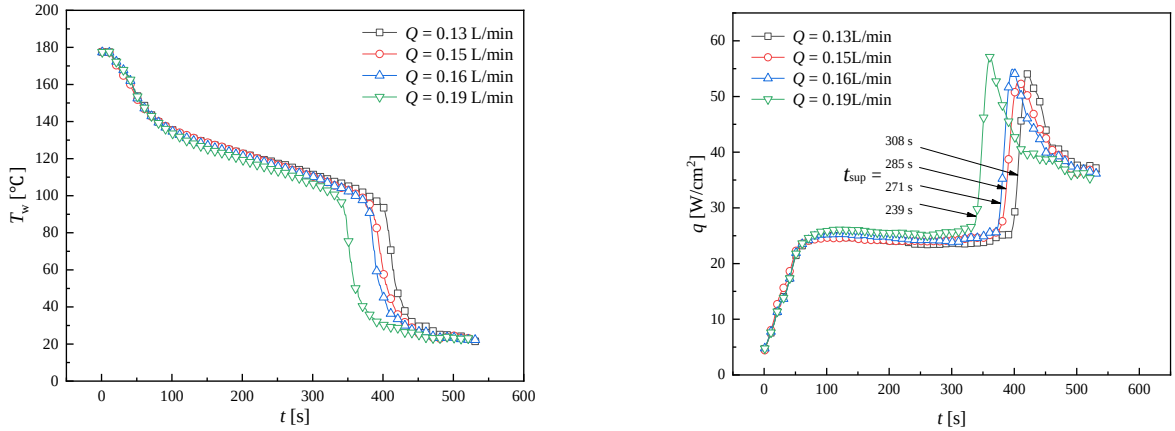

(a) Variations of top surface temperature (b) Variations of heat flux

Fig. 8 Variations of top surface temperature and heat flux with different flow rate

Fig. 8 shows that the time of reaching STD point reduces slightly with the increase of flow rate. As the flow rate rises from 0.13 to 0.19 L/min, the time of reaching STD point is about 56 s ahead of that.

Besides, STD point of transient spray cooling without heat source is not affected by the flow rate, and it maintains about 100.6 ℃ in this experiment. The time of reaching CHF also reduces due to the increase of the flow late. The maximum CHF in this condition is about 57.11 W/cm^2.The vapor film suppressed time t_{sup} reduces about 69 s which is from 308 to 239 s.

In the investigation of flow rate, the flow rate of R134a may possibly have negative influence on vapor film. In the film boiling stage, the formation of vapor film is greatly disturbed with the increase of the flow rate. These results in a slight increase of q and a little reduce of t_{sup}.

4.3. Effect of sub-cooling on heat transfer process

In the experiment, by adjusting the water flow rate of the condenser to change the sub-cooling of R134a, the effect of sub-cooling temperature T_{sc} (which is the difference between T_{in} and T_{out}) on the transient spray cooling are studied.

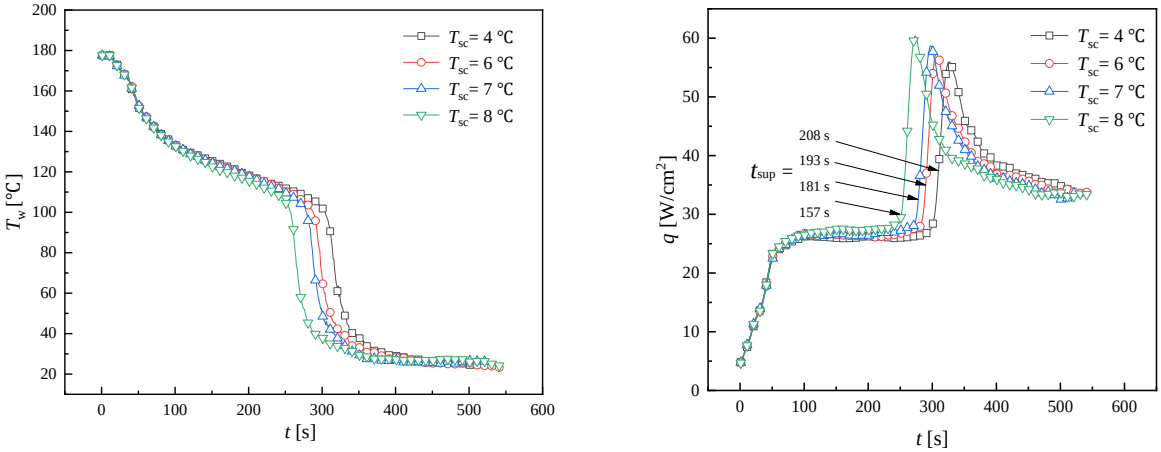

(a) Variations of top surface temperature (b) Variations of heat flux

Fig. 9 Variations of top surface temperature and heat flux with different sub-cooling

As Fig. 9 shows, with the increase of the sub-cooling, the time of reaching STD point is slightly reduced. As $\boldsymbol{T_{sc}}$ increases from 4 to 8 ℃, the time of reaching STD point is about 48 s ahead of that. Besides, STD point is also hardly related with $\boldsymbol{T_{sc}}$ and maintains about 100.8 ℃ in this experiment. CHF rises while the time of reaching CHF reduces due to the increase of temperature $\boldsymbol{T_{sc}}$. The maximum CHF in this condition is about 60.36 W/cm^2.The vapor film suppressed time $\boldsymbol{t_{sup}}$ reduces about 51 s which is from 208 to 157 s. As the increase of $\boldsymbol{T_{sc}}$, the heat flux in film boil stage increases, that is because the lower spray temperature suppressed the formation of vapor film. These results in a slight increase of q and a little reduce of $\boldsymbol{t_{sup}}$.

4.4. Effect of chamber pressure on heat transfer process

By adjusting the charge of R134a to improve the chamber pressure P_c, the effect of P_c on the transient spray cooling are studied.

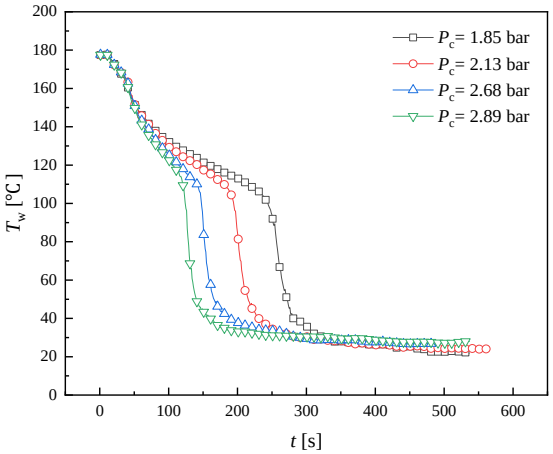

(a) Variations of top surface temperature

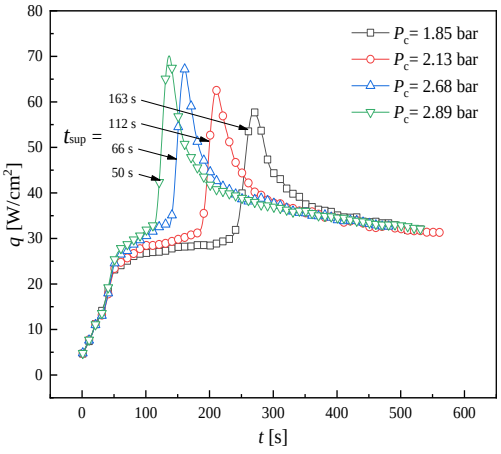

(b) Variations of heat flux

Fig. 10 Variations of top surface temperature and heat flux with different chamber pressure

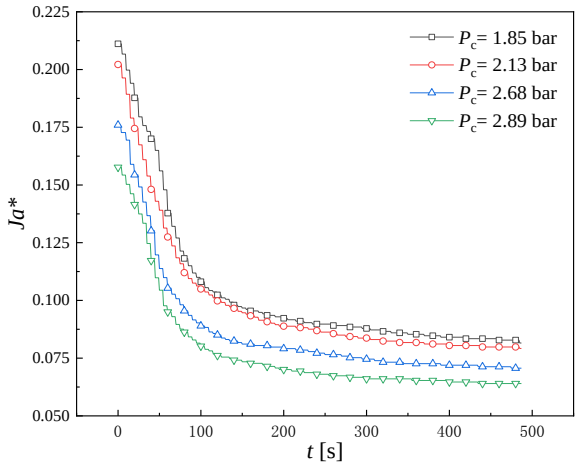

Fig.11 Variations of Ja with different chamber pressure

Tab.2

Properties of R134a under different chamber pressure

P_c (bar)	T_{sc} (°C)	ρ (kg/m^3)	C_p (kJ/kg°C)	μ (mPa s)	λ (W/m°C)	γ kJ/kg	Pr
1.85	-12.03	1333.5	1.312	0.312	0.0971	207.41	4.196
2.13	-8.47	1322.3	1.319	0.297	0.0958	204.87	4.097
2.68	-2.42	1302.7	1.335	0.275	0.0931	200.43	3.942
2.89	-0.36	1296.0	1.340	0.268	0.0922	198.88	3.893

As shown in Figure 10, with the increase of P_c, the time of reaching STD point is reduced significantly. As P_c increase from 1.85 to 2.89 bar, the time of reaching STD point is about 108 s ahead of that. Compared with T_{sc} and Q, the STD point increases with the increase of P_c, which rises from 95 to 112℃. The CHF rises while the time of reaching it reduces due to the increase of P_c. The maximum CHF in this condition is about 70.08 W/cm^2. The vapor film suppressed time t_{sup} reduces about 113 s which is from 163 to 50 s.

In order to investigate the influence mechanism of chamber pressure, Table 2 lists the properties of

R134a under different chamber pressure. As shown in Table 2, with the increase of chamber pressure, *Pr* changes very little. Therefore, the variations in the thermophysical properties of R134a can be negligible. Meanwhile, the transient Jacob number Ja^* under different chamber pressure is shown in Figure 11. From Fig 11, it can be seen that Ja^* decreases obviously as the spray cooling goes. What's more, Ja^* decreases visually with the increases of P_c. As the decrease of Ja^*, the growth of vapor film was inhibited, so the heat transfer is enhanced. Furthermore, the transition from film boiling to nuclear boiling could be promoted. This is a critical for improving spray cooling rate.

5. Conclusions

In this study, the heat transfer characteristics and influencing factors of a closed-loop transient spray cooling were investigated. The spray cooling curve was built accurately. From the analytical and experimental investigations, the following conclusions are drawn:

(1) Closed-loop transient spray cooling curve contains four stages: start-up stage, film boiling stage, transition boiling stage and nucleate boiling stage. The vapor film suppressed time t_{sup} is the main period that the spray cooling should pass through.

(2) In the range of the experiment, the STD and CHF change little with the variations of flow rate and sub-cooling. The increase of flow rate and sub-cooling has limited effect on cooling rate as well. On the contrary, the cooling rate can be significantly increased with the increase of chamber pressure. The STD and CHF increases with the rise of chamber pressure. The maximum CHF is 70.08 W/cm^2 in this experiment.

(3) The transient Jacob number Ja^* decreases with the increases of chamber pressure. *Ja* represents the superheat of vapor film in boiling heat transfer. As the decrease of Ja^*, the growth of vapor film is inhibited, furthermore, the transition from film boiling to nuclear boiling could be promoted.

Acknowledgement

The authors gratefully acknowledge the Natural Science Foundation of Jiangsu Province in China (No. BK20180960).

Nomenclature

c_p	specific heat capacity [kJ/kg℃]
h	heat transfer coefficient [W/cm^2℃]
P	pressure [bar]
q	heat flux [W/cm^2]
Q	flow rate[L/min]
t	time [s]
T	temperature [℃]

Greek

γ	Latent heat of evaporation [kJ/kg]
δ_1	distance between T_1 and T_2 [mm]
δ_2	distance between T_w and T_1 [mm]
λ	heat conductivity [W/m℃]

μ	dynamic viscosity coefficient [Pa s]
ρ	density [kg/m^3]
Δt	onetime step [s]
ΔT_1	temperature difference of Δt [℃]

Subscripts

c	chamber
in	condenser inlet
lh	latent heat
out	nozzle outlet
sat	saturation
sc	sub-cooling
sup	suppress
w	top surface

References

[1] Cheng W.L., Zhang W.W., Chen H., Hu L., Spray cooling and flash evaporation cooling: The current development and application. *Rene. Sustain. Energy Reviews, 55* (2016) pp. 614-628

[2] Cheng W.L., Liu Q.N., Zhao R., Fan H.L., Experimental investigation of parameters effect on heat transfer of spray cooling. *Int. J. Heat Mass Transf., 46* (2010), 8, pp. 911-921

[3] Zhao R., Cheng W. L., Liu Q.N., Fan H.L., Study on heat transfer performance of spray cooling: model and analysis. *Int. J. Heat Mass Transf., 46* (2010), 8, pp. 821-829

[4] Estes K.A., Mudawar I., Comparison of two-phase electronic cooling using free jets and sprays. *J. Electron Packag., 117* (1995), pp. 323-332

[5] Kandlikar SG, Bapat AV, Evaluation of jet impingement, spray and micro-channel chip cooling options for high heat flux removal. *Heat Transf. Eng., 28* (2007), pp. 911-923

[6] Xu J.G., Cui J.J., Dong N.N., Cao L., Transient spray cooling system for high-power laser treatment. *Optics Precision Eng, 27* (2019), 6, pp. 1309-1317

[7] Cen Q.G., Wang Z.T., Wen J.L., Experimental study on spray characteristics for metal cutting by PDA. *J. Drainage Irrigation Machinery Eng., 25* (2007), 3, pp. 53-56

[8] Z Ling., Zhang Z., Shi G., Fang X., Wang L., Gao X., Fang Y., Review on thermal management systems using phase change materials for electronic components, Li-ion batteries and photovoltaic modules. *Rene. Sustain. Energy Reviews, 31* (2014), pp. 427–438

[9] Zheng Y., Yang Y., Zhao X., Gong W., Research Process on Spectral Beam Combinging Technology of High-Power Fiber Lasers. *Chinese J. Lasers, 44* (2017), 2, pp. 35-50

[10] Cabrera E.A., Heat flux correlation for spray cooling in the nucleate boiling regime. *Exp. Heat Transf., 16* (2003), 1, pp. 19-44

[11] Xie J., Tan Y., Duan F. Ranjith K., Wong T., Toh K, Study of heat transfer enhancement for structured surfaces in spray cooling. *Appl. Therm. Eng., 59* (2013), pp. 464-472

[12] Chen R.H., Chow L.C., Navedo J.E., Effects of spray characteristics on critical heat flux in subcooled water spray cooling. *Int. J. Heat Mass Transf. 45* (2002), 19, pp. 4033–4043

[13] Peng C., Xu X., Liang X., Experimental study on temperature variation patterns and deterioration of spray cooling with R21. *Int. J. Heat Mass Transf., 121* (2018), pp. 1159-1167

[14] Hsieh S.S., Fan T.C., Tsai H.H., Spray cooling characteristics of water and R-134a. Part II: transient cooling. *Int. J. Heat Mass Transf.*, *47* (2004), 26 pp. 5713-5724
[15] Liu N., Li L.R., Zhong Z.M., Experimental study on spray cooling performance of microstructure surface. *J. Mechan. Eng.*, *53* (2017), 6, pp. 158-165
[16] Cao L., Chen J.N., Jiang P.X., Xu N.N., Experimental study on closed spray cooling system based on refrigeration cycle. *J. Eng. Therm.*, *39* (2018), 2, pp. 373-378
[17] Lu S., Wang Y.X., Y Shen.F., Sun P., Xiao M.J., Numerical simulation study on heat transfer characteristics of spray cooling in single-phase region, *Therm. Sci. Tech.*, *16* (2017), 01, pp. 34-39
[18] Liu H., He Y., Cai C., Takaku R., Yin H.C., Effects of ethanol and n-butanol additives on spray cooling. *J. Chemical Industry Eng.*, *70* (2019), 1, pp. 65-71
[19] Rini DP., Chen R.H., Chow L.C., Bubble behavior and heat transfer mechanism in FC-72 pool boiling. *Exp. Heat Transf.*, *14* (2001), pp. 27-44
[20] Rini DP., Chen R.H., Chow L.C., Bubble behavior and nucleate boiling heat transfer in saturated FC-72 spray cooling, *J. Heat Transf.*, *124* (2002), pp. 63-72
[21] Tian J.M., Chen B., Li D., Zhou Z.F., Transient spray cooling: Similarity of dynamic heat flux for different cryogens, nozzles and substrates. *Int.J. Heat Mass Transf.*, *108* (2017), pp. 561-571
[22] Liu P., Kandasamy R., Feng H., Wong T., Toh K. Influence of air on heat transfer of a closed-loop spray cooling system. *Exp. Therm Fluid Sci.*, 2020, 190903. DOI: https://doi.org/10.1016/j.expthermflusci.2019.109903
[23] Wang R., Z Zhou., Chen B., Bai F., Wang G., Surface heat transfer characteristics of R404A pulsed spray cooling with an expansion-chambered nozzle for laser dermatology, International *Int. J. Refrigeration*, *60* (2015), pp. 206-216
[24] Karwa N., S Kale.R., Subbarao P.M.V., Experimental study of non-boiling heat transfer from a horizontal surface by water sprays. *Exp. Therm. Fluid Sci.*, *32* (2007), pp. 571–579
[25] Estes K.A., Mudawar I., Correlation of Sauter mean diameter and critical heat flux for spray cooling of small surfaces. *Int. J. Heat Mass Transf.*, *38* (1995), 16, pp. 2985-2996
[26] Zhao Y.X., Zhao X., Zhang B., Yin Z.C., Solution of thermal boundary conditions using inverse heat conduction problem in intermittent spray cooling. *J. Dalian University of Tech.*, *59* (2019), 04, pp. 359-365

Submitted: 25.08.2020.
Revised: 25.11.2020
Accepted: 08.12.2020.